Avrupa Bilim ve Teknoloji Dergisi
Sayı 21, S. 402-409, Ocak 2021
© Telif hakkı EJOSAT'a aittir
Araştırma Makalesi

www.ejosat.com ISSN:2148-2683

European Journal of Science and Technology
No. 21, pp. 402-409, January 2021
Copyright © 2021 EJOSAT
Research Article

Quadrature Spatial Pulse Amplitude Modulation and Generalized Versions for VLC

Yasin Çelik[1*]

[1*] Aksaray University, Faculty of Engineering, Department of Electrical and Electronics, Aksaray, Turkey (ORCID: 0000-0001-8972-9970), yasincelik@aksaray.edu.tr

(First received 11 September 2020 and in final form 28 January 2021)

(**DOI:** 10.31590/ejosat.793791)

ATIF/REFERENCE: Celik, Y. (2021). Quadrature Spatial Pulse Amplitude Modulation and Generalized Versions for VLC. *European Journal of Science and Technology*, (21), 402-409.

Abstract

Quadrature spatial modulation (QSM) is a promising technique for multiple-input-multiple-output (MIMO) systems that completely prevents inter-channel interference (ICI) and provides spatial multiplexing gain greater than spatial modulation (SM). In QSM, the information conveyed by the indices of the transmit antennas doubles thanks to the in-phase and quadrature components. In this regard, the quadrature spatial pulse amplitude modulation (QSPAM), which enables QSM for visible light communication (VLC) with the help of orthogonal pulses, is proposed in this paper. Generalized versions of QSPAM, i.e. generalized QSPAM (GQSPAM) and variable-length generalized QSPAM (VGQSPAM) have also been proposed and a well-known scheme, spatial pulse amplitude modulation (SPAM), is used as a benchmark. The proposed schemes efficiently use the spatial domain and increase spectral efficiency with fewer light-emitting diodes (LEDs). The angular diversity receiver (ADR) proposed for the channel correlation problem of indoor MIMO VLC systems is used as the receiver unit. Although ADR reduces channel correlation, it is not sufficient in the corner of the room. Therefore, a precoding matrix is generated with the help of convex optimization for demanding conditions. The bit error rate (BER) performance of considered modulation schemes is obtained through Monte Carlo simulations and, the upper bound BER performances are also derived analytically to validate these results. Additionally, spectral efficiency (SE) versus signal-to-noise ratio (SNR) graphs are obtained at a fixed symbol error rate (SER) of 10^{-5}. According to the results, VGQSPAM performs better than the other schemes and benchmarks when the channel correlation is low. However, GQSPAM outperforms VGQSPAM for harsh conditions.

Keywords: VLC, MIMO, Spatial Modulation.

Görünür Işık Haberleşmesi için Dörtlü Uzamsal Darbe Genlik Modülasyonu ve Genelleştirilmiş Versiyonları

Öz

Dörtlü uzamsal modülasyon (DUM), kanallar arası girişimi (KAG) tamamen önleyen ve uzamsal modülasyondan (UM) daha fazla çoğullama kazancı sağlayan bir modülasyon planı olarak çok-girişli çok-çıkışlı (ÇGÇÇ) sistemler için ümit verici bir tekniktir. DUM'da, verici antenlerin indisleri tarafından iletilen bilgiler, eş fazlı ve karesel bileşenler sayesinde iki katına çıkar. Bu bağlamda, bu yazıda, ortogonal darbeler yardımıyla görünür ışık haberleşmesi (GIH) için DUM'yi mümkün kılan dörtlü uzamsal darbe genlik modülasyonu (DUDGM) önerilmiştir. Bu çalışmada aynı zamanda, DUDGM'nin genişletilmiş çeşitleri olan genelleştirilmiş DUDGM (GDUDGM) ve değişken uzunluklu genelleştirilmiş DUDGM (VGDUDGM) da önerilmiştir. İyi bilinen bir modülasyon planı olan, uzamsal darbe genlik modülasyonu (UDGM) performans kıyaslaması yapmak için kullanılmıştır. Önerilen şemalar, uzamsal alanı

[*] Aksaray University, Faculty of Engineering, Department of Electrical and Electronics, Aksaray, Turkey (ORCID: 0000-0001-8972-9970), yasincelik@aksaray.edu.tr

verimli bir şekilde kullanır ve daha az ışık yayan diyot (LED) ile spektral verimliliği artırır. İç mekan ÇGÇÇ GIH sistemlerinin kanal korelasyon problemi için önerilen açısal çeşitlemeli alıcı (AÇA), alıcı ünite olarak kullanılmıştır. AÇA kanal korelasyonunu azaltmasına rağmen odanın köşesinde yeterli değildir. Bu nedenle, zorlu koşullar için dışbükey optimizasyon yardımı ile bir ön kodlama matrisi oluşturulmuştur. Değerlendirilen modülasyon şemalarının bit hata oranı (BHO) performansı, Monte Carlo simülasyonları yoluyla elde edilmiş ve üst sınır BER performansları da bu sonuçları doğrulamak için analitik olarak türetilmiştir. Ek olarak, spektral verimlilik (SV) ve sinyal-gürültü oranı (SGO) grafikleri, 10^{-5} sabit sembol hata oranında (SHO) elde edilmiştir. Sonuçlara göre, VGDUDGM, kanal korelasyonu düşük olduğunda diğer önerilen şemalardan ve UDGM'den daha iyi performans gösterir. Bununla birlikte, GDUDGM zorlu koşullar için VGDUDGM 'den daha iyi performans göstermiştir.

Anahtar Kelimeler: Görünür ışık haberleşmesi (GIH), Çok-girişli çok-çıkışlı (ÇGÇÇ), Uzamsal modülasyon (UM).

1. Introduction

The use of multiple light emitting diodes (LEDs) and photo-detectors (PDs) enables multiple-input multiple-output (MIMO) techniques for visible light communication (VLC). In [1], the traditional MIMO technique, where data streams are transmitted from all antennas simultaneously, was studied for indoor VLC. This technique, which is called spatial multiplexing (SMX), increases the spectral efficiency (SE) linearly with the number of LEDs on the transmitter (Tx) side. However, the improvement of SE on the Tx side has a trade-off with inter-channel interference (ICI) on the receiver side (Rx). Furthermore, the energy efficiency (EE) of this technique is low due to multiple radio frequency (RF) chains [2].

Space modulation techniques (SMTs) have been proposed as another MIMO technology that improves the SE by transmitting additional data bits via the indices of the components of the transceiver system. In these schemes, the EE of the system is increased by limiting the number of required RF chains in a symbol period [2]. In [3], quadrature spatial modulation (QSM), which can double the information carried by the indices, was proposed as a promising SMT scheme. Interference of QSM signals is prevented due to the orthogonality between the in-phase and quadrature components. Furthermore, generalized structures were proposed to avoid the restriction in the number of Tx antennas, which should have a power of two [4]-[6].

The intensity modulation direct detection (IM/DD) technique, which uses only real and positive signals to emit data, is often used in VLC because of incoherent nature of LEDs. Since complex and negative signals are included, the QSM scheme cannot be used directly in VLC systems [7]. It can be adapted to VLC with the help of a DC signal, but the DC signal decreases the EE of the system. On the other hand, pulse modulation schemes i.e., pulse position modulation (PPM), pulse amplitude modulation (PAM) and pulse position and amplitude modulation (PPAM), are more suitable for VLC systems as they have real signals [8]-[10]. However, since they have a one-dimensional signal space, the QSM scheme cannot be enabled for VLC with these modulations.

In this paper, we propose a new QSM scheme for VLC, which we call quadrature spatial pulse amplitude modulation (QSPAM). In this scheme, two orthogonal pulses are used, each having a PAM modulation. Generalized versions of QSPAM are also proposed as generalized QSPAM (GQSPAM) and variable-length generalized QSPAM (VGQSPAM). The advantages of QSPAM and generalized versions are written as follows;

- They are applied directly to VLC with the help of orthogonal PAM signals.
- Thanks to the general SM structure, they can be implemented with a single modulation circuit. This feature increases the EE of the transciever system.
- Spatially modulated bits are doubled in QSPAM. Therefore, the SE of the QSPAM can be given as $(\log_2(M) + 2\log_2(N_t))$ bit per channel use (bpcu) where M and Nt are the constellation size and the number of LEDs, respectively.
- GQSPAM and VGQSPAM are also use the spatial domain more efficiently. The SE of GQSPAM is written as $\log_2(M) + 2\lfloor \log_2 \binom{N_t}{N_a} \rfloor$ bpcu, where $\lfloor\rfloor$ stands for ceiling operator and N_a denotes the number of active LEDs. Moreover, the SE of VGQSPAM is given as $\log_2(M) + 2(N_t - 1)$ bpcu.

2. Material and Method

2.1. System Model

In this paper, an indoor MIMO VLC system using non-coherent LEDs and an angular diversity receiver (ADR) is considered [11]. Room geometry is demonstrated in Figure 1, where ADR and room sizes are not scaled to better visualize the ADR structure. The number of LEDs is represented by N_t. At the receiver side, N_r = 4 PDs are placed on the ADR and the received signal vector with length $N_r \times 1$ is given as follows,

$$\mathbf{y} = \eta\rho\mathbf{H}\mathbf{W}\mathbf{x} + \mathbf{n}, \quad (1)$$

where, without losing generality, we assume that the product of the electrical-to-optical conversion coefficient (η) and the photo-detector sensitivity (ρ) is one. The noise affecting the signal at the receiver is modeled as additive white Gaussian noise (AWGN) which is independent of the transmitted signal and added to the received signal in the electrical domain [12]. Thus, each element of **n** is a zero mean Gaussian random variable with a variance of $\sigma^2 = N_0/2$ per dimension. **x** is the transmitted signal vector and **W** indicates the precoding matrix with dimensions $N_t \times N_t$ described in the next section.

H is the channel matrix and h_{ij} represents the respective channel coefficient of the indoor VLC link between the j^{th} LED and the i^{th} PD. These links are assumed to have non-line of sight (NLOS) components up to three reflections as well as a line of sight (LOS), so the channel coefficient, h_{ij}, is obtained as follows,

$$h_{ij} = h_{ij}^{LOS} + h_{ij}^{NLOS}. \quad (2)$$

It is assumed that the LEDs on the ceiling have a *Lambertian* emission characteristics, thus the LOS coefficient, h_{ij}^{LOS}, can be given as follows,

$$h_{ij}^{\mathrm{LOS}} = \begin{cases} \dfrac{(m+1)A}{2\pi d_{ij}^2} cos^m(\alpha_{ij})\cos(\beta_{ij}), & \left|\dfrac{\beta_{ij}}{FOV}\right| \le 1, \\ 0, & otherwise, \end{cases} \quad (3)$$

here, d_{ij} is the distance in meters between the j^{th} LED and the i^{th} PD. *FOV* is the field of view angle of the PDs. Walls, ceilings and floors are often rough according to the light wavelength, so the reflection of the light is diffuse. Therefore, the differential areas on the surfaces have a *Lambertian* emission pattern, as well [12]. NLOS that comes out of the j^{th} LED and reaches the i^{th} PD at the end of k reflection can be written as follows [12],

$$h_{ij}^{\mathrm{NLOS(k)}} = \begin{cases} \Lambda_{ij}^{(1)}\Lambda_{ij}^{(2)} \dots \Lambda_{ij}^{(k+1)}, & \left|\dfrac{\beta_{ij}^{(k+1)}}{FOV}\right| \le 1, \\ 0, & otherwise. \end{cases} \quad (4)$$

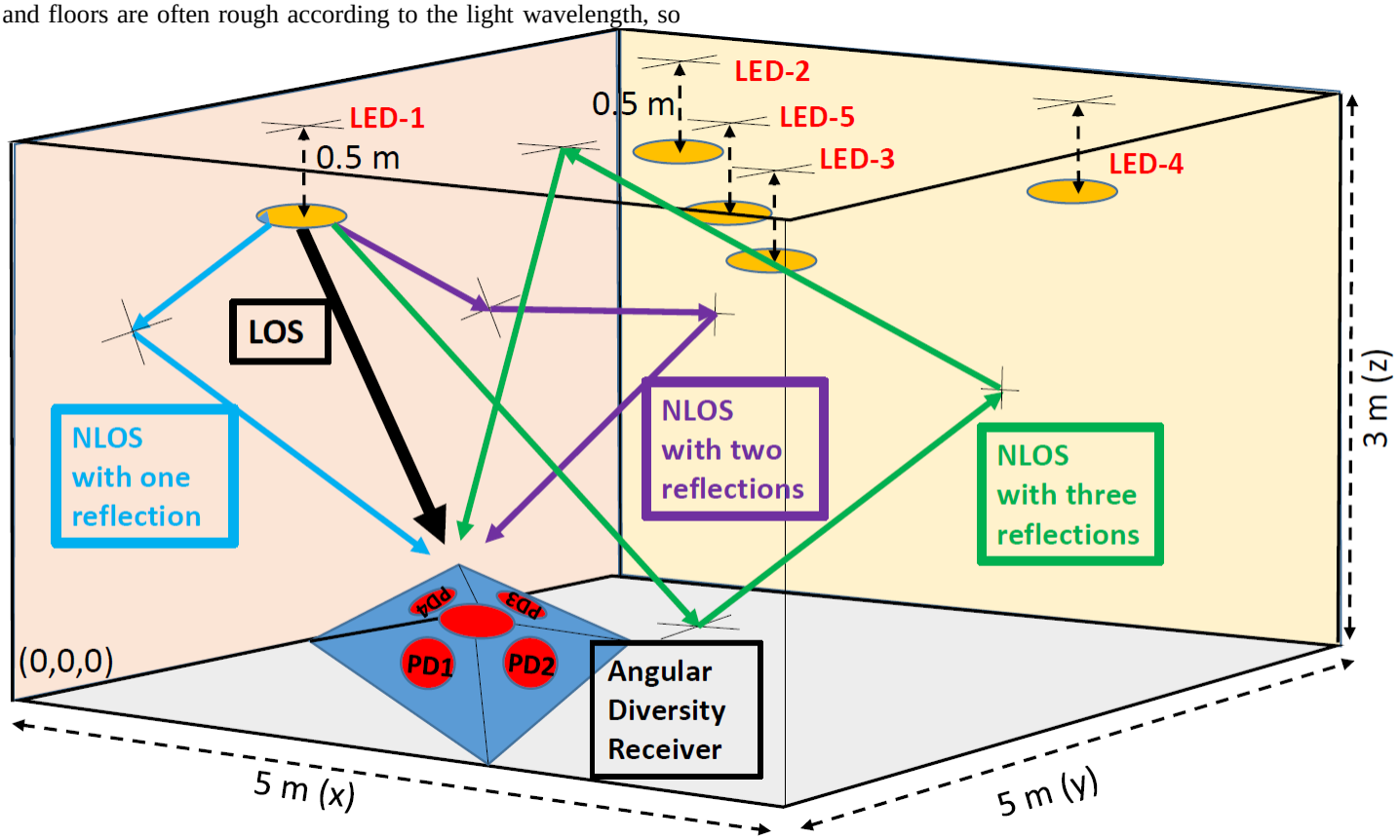

Figure 1. Room geometry with N_t = 5 LEDs and an ADR including LOS and NLOS link examples from LED-1.

where $\Lambda^{(n)}$, which was given in [12], is the fading coefficient of the link between *(n-1)*th and *n*th surfaces, where *zeroth* surface is LED and *(n+1)*th surface is PD. Finally, h_{ij}^{NLOS} can be written as,

$$\mathrm{h}_{\mathrm{ij}}^{\mathrm{NLOS}} = \sum_{S}\sum_{k=1}^{3} \mathrm{h}_{ij}^{\mathrm{NLOS(k)}}, \quad (5)$$

where *S* is the set of differential areas. These areas are determined as 0.2m x 0.2m square surfaces on the walls, ceiling, and floor. Thus, the set *S* is the interior surface area of the room. As mentioned above, these surfaces act as a *Lambert* source and reflect the intensity falling relative to the reflection coefficient. These coefficient values are assumed as in [12]. Indoor VLC channels have a large coherence bandwidth, so the system under consideration has no inter-symbol interference (ISI) and synchronization is assumed to be perfect [13]. All parameters considered in this study are given in Table 1.

The transmitted signal vector is denoted by $\mathbf{x} = [x_1 \dots x_{Nt}]^T$. Depending on the corresponding modulation i.e. QSPAM, GQSPAM, and VGQSPAM and incoming data bits, the active LEDs are determined. These modulations follow the same procedure as in [14] to identify the active LEDs.

In Fig. 2, system model for QSPAM is shown. The signal constellation consists of two-dimension is shown in Fig. 2a, so the modulated signal contains two perpendicular unipolar PAM signals. Therefore, proposed schemes have two base signals as seen in Fig. 2b. An example of bit mapping and transmitted signal for the bit stream "110001" is demonstrated in Fig. 2c and Fig. 2d, respectively.

Table 1. Parameters of the Considered VLC System

Room dimensions (XxYxZ)	5x5x3 (m)
No. of Transmitters (N_t)	4 and 5
LED distance from the ceiling	0.5 (m)
Semi-angle at half power ($\Phi_{1/2}$)	60°
Lambertian order (m)	1
ADR height from the floor	0.85 (m)
Elevation of PDs	60°
Azimuth of ADR	45°
Responsivity (R)	0.4 (A/W)
Area of a PD (A)	$1x10^{-4}$ (m^2)
Field of view of PDs (FOV)	70°
Wall reflectivity coefficient (ρ_w)	0.8
Ceiling reflectivity coefficient (ρ_c)	0.5
Floor reflectivity coefficient (ρ_f)	0.3
Area of differential elements (dA)	0.04 (m^2)
ADR (x,y) position (Center)	{2.50, 2.50}
ADR (x,y) position (Corner)	{0.50, 0.50}
LED (x,y) positions (N_t=4)	{1.25, 1.25; 1.25, 3.75; 3.75, 1.25; 3.75, 3.75}
LED (x,y) positions (N_t=5)	{1.03, 1.03; 3.96, 1.03; 2.50, 2.50; 1.03, 3.96; 3.96, 3.96}

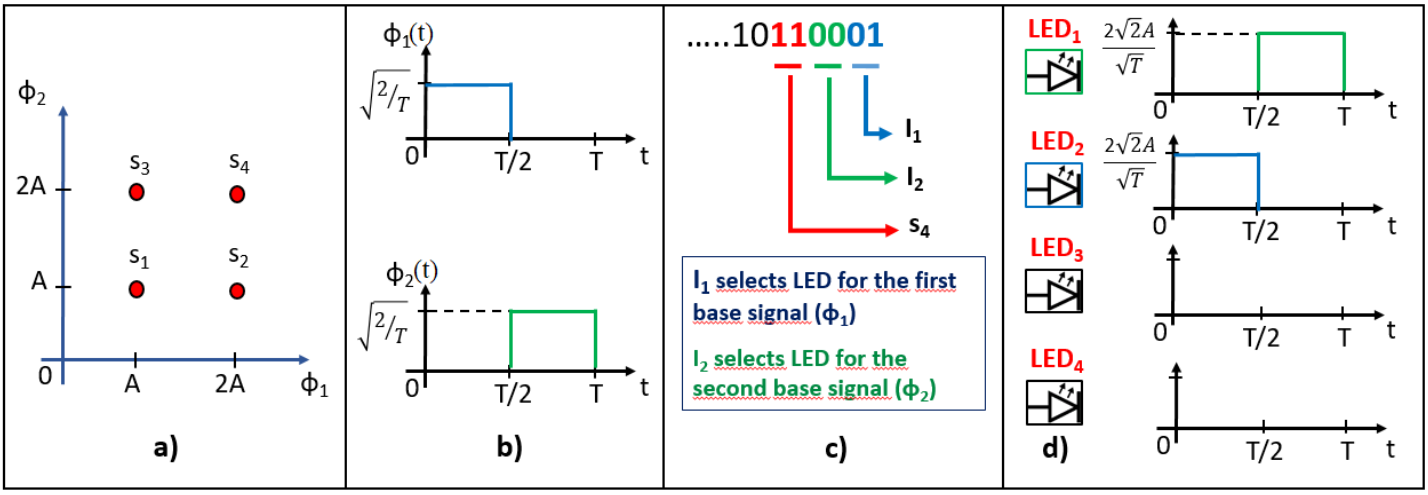

Figure 2. System model for QSPAM with 4 LEDs: ***a)*** *signal constellation for M=4,* ***b)*** *base signals (ϕ_1 and ϕ_2),* ***c)*** *bit mapping,* ***d)*** *transmitted signal for the bit stream "110001".*

Briefly according to I_1 and I_2, active LEDs are determined for the schemes considered, and the symbol corresponding to the data bits is transmitted through the active LEDs. As another example, if the incoming bit stream is "011010", the first two bits (10) activate the LED3 for the base signal $\phi_1(t)$, the following two bits (10) activate the LED3 for the base signal $\phi_2(t)$ and the last two bits (01) select the symbol s_2. An example of bit-to-active LED mapping for the QSPAM and GQSPAM schemes is shown in Table 2. In this table, 4 LEDs on the Tx side are considered and the number of active LEDs (N_a) is selected as 2 for the GQSPAM scheme. Moreover, x_1 is the transmitted signal comprised of $\phi_1(t)$ base signal and similarly, x_2 is the transmitted signal comprised of $\phi_2(t)$ base signal. In the VGQSPAM scheme with 4 LEDs, this mapping is performed with 6 bits, where half of them select the LED or LEDs for the signal comprised of the first base signal and the other half selects the LED or LEDs for the signal comprised of the second.

Detailed information for the mapping procedure is available in [14].

Maximum likelihood (ML) receiver is considered at the receiver to obtain the transmitted signal vector, **x**, assuming all the constellation symbols are equally likely. The noisy signal at the output of the PDs is the input of the ML detector. Thus, the estimated vector, $\hat{\boldsymbol{x}}$, can be written as follows,

$$\hat{\mathbf{x}} = \underset{\mathrm{x}}{\operatorname{argmin}}\left(\left|\left|\mathbf{y} - \mathbf{HWx}\right|\right|_{\mathrm{F}}^{2}\right), \tag{6}$$

where *F* denotes the Frobenious norm. We assume that the channel state information (CSI) and precoding matrix is known at both Tx and Rx.

Table 2. Bit-to-Active LEDs Mapping for the Schemes Under Consideration (N_t=4).

Incoming Bits		**Active LEDs**							
I_1	I_2	***QSPAM***				***GQSPAM*** *(N_a = 2)*			
		LED1	***LED2***	***LED3***	***LED4***	***LED1***	***LED2***	***LED3***	***LED4***
00	00	x_1+x_2				x_1+x_2		x_1+x_2	
00	01	x_1	x_2			x_1+x_2		x_1	x_2
00	10	x_1		x_2		x_1	x_2	x_1+x_2	
00	11	x_1			x_2	x_1	x_2	x_1	x_2
01	00	x_2	x_1			x_1+x_2		x_2	x_1
01	01		x_1+ x_2			x_1+x_2			x_1+x_2
01	10		x_1	x_2		x_1	x_2	x_2	x_1
01	11		x_1		x_2	x_1	x_2		x_1+x_2
10	00	x_2		x_1		x_2	x_1	x_1+x_2	
10	01		x_2	x_1		x_2	x_1	x_1	x_2
10	10			x_1+x_2			x_1+x_2	x_1+x_2	
10	11			x_1	x_2		x_1+x_2	x_1	x_2
11	00	x_2			x_1	x_2	x_1	x_2	x_1
11	01		x_2		x_1	x_2	x_1		x_1+x_2
11	10			x_2	x_1		x_1+x_2	x_2	x_1
11	11				x_1+x_2		x_1+x_2		x_1+x_2

2.2. Precoding and Average Bit Error Rate

ADR is a compact solution proposed for the channel correlation problem of indoor MIMO VLC systems. However, it does not provide the best channel condition all over the room, especially near the corner position. Therefore, in this study, a diagonal precoder matrix, **W**, is obtained for the channel matrix, **H,** in order to reduce the channel correlation. The problem of optimizing the diagonal precoder matrix can be modeled as a convex optimization problem and the objective function can be written as [15],

$$\begin{aligned}\widehat{\mathbf{W}} &= \underset{i,j}{\operatorname{argmax}}\left(min\left(\left|\left|\mathbf{HW}\left(\mathbf{x}_{\mathrm{i}} - \mathbf{x}_{\mathrm{j}}\right)\right|\right|_{F}^{2}\right)\right), \quad i \neq j,\\ &= \underset{i,j}{\operatorname{argmax}}\left(min\left(\left(\mathbf{x}_{\mathrm{i}} - \mathbf{x}_{\mathrm{j}}\right)^{H}\mathbf{W}^{\mathbf{H}}\mathbf{H}^{\mathbf{H}}\mathbf{HW}\left(\mathbf{x}_{\mathrm{i}} - \mathbf{x}_{\mathrm{j}}\right)\right)\right), \\ &= \underset{i,j}{\operatorname{argmax}}\left(min\left(\mathbf{w}^{\mathbf{H}}\mathbf{U}_{\mathrm{ij}}\mathbf{w}\right)\right), \qquad i \neq j,\end{aligned} \tag{7}$$

where **w** is a column vector formed by diagonal of **W** and $\mathbf{U}_{\mathrm{ij}} = \mathbf{H}^{\mathbf{H}}\mathbf{H} \odot \left(\left(\mathbf{x}_{\mathrm{i}} - \mathbf{x}_{\mathrm{j}}\right)\left(\mathbf{x}_{\mathrm{i}} - \mathbf{x}_{\mathrm{j}}\right)^{H}\right)^{T}$. Here, $\odot$ represents the Hadamard product. Finally, the *max-min* problem after convex relaxation can be written as follows [16],

$$\begin{aligned}&\underset{w}{\operatorname{argmax}} \quad t,\\ &subject\ to \quad t \leq 2\mathbf{w}_k^H\mathbf{U}_{\mathrm{ij}}\mathbf{w} - \mathbf{w}_k^H\mathbf{U}_{\mathrm{ij}}\mathbf{w}_k, \quad i \neq j,\\ &||w||^2 \leq P_{max}\ ,\\ &w > 0,\end{aligned} \tag{8}$$

where $\mathbf{w}_{\mathrm{k}}$ is a column vector with arbitrary initial values and P_{max} indicates a value associated with the maximum operating current of the LED. The convex optimization problem can be solved with the help of the CVX toolbox [1

ADR provides the best channel condition in the center of the room, so the precoding matrix is obtained as the identity matrix. However, correlation between the channels increases near the corner. Diagonal elements of the precoding matrices obtained for the corner position are given in Table 3, where the channel matrices are normalized with 10^{-5}.

The average bit error rate (ABER) performance of the proposed schemes are obtained by using pairwise error probability (PEP), which is given as follows

$$\begin{aligned}&P(\mathbf{x}_m \to \mathbf{x}_m)\\ &= \Pr(||\mathbf{y} - \mathbf{HWx}_m||_{\mathrm{F}}^2 > ||\mathbf{y} - \mathbf{HWx}_n||_{\mathrm{F}}^2 \mid \mathbf{H}, \mathbf{W}),\\ &= \Pr(2Re\{\mathbf{nHW\Gamma}\} > ||\mathbf{HW\Gamma}||_{\mathrm{F}}^2 \mid \mathbf{H}, \mathbf{W}),\\ &= Q\left(\sqrt{\frac{||\mathbf{HW\Gamma}||_{\mathrm{F}}^2}{2N_0}}\right),\end{aligned} \tag{9}$$

where Q-function is the tail probability of the standard normal distribution and the vector $\mathbf{\Gamma}$ represents $\mathbf{x_m} - \mathbf{x_n}$. Finally, the upper bound ABER is given as follows,

$$P_{ABER} \leq \frac{1}{\xi 2^{\xi}} \sum_{m=1}^{2^{\xi}} \sum_{n=1}^{2^{\xi}} P(\mathbf{x}_m \rightarrow \mathbf{x}_m)\, d_{mn}^{T}, \qquad (10)$$

here ξ is the SE of the proposed system which is $\log_2(MN_t^2)$ bpcu and d_{mn}^{T} denotes the Hamming distance between m^{th} and n^{th} code-words.

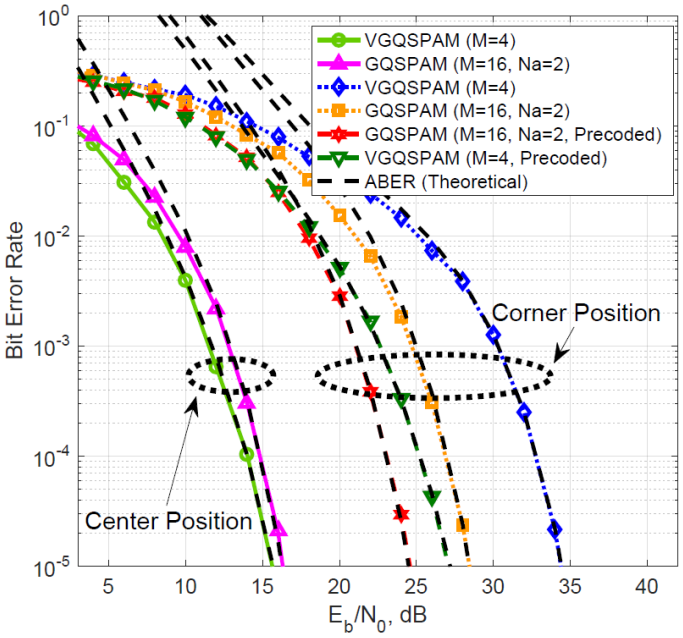

Figure 3. BER simulations and ABER theoretical results for 4 LEDs in two different Rx positions at a spectral efficiency of 4 bits/sec/Hz.

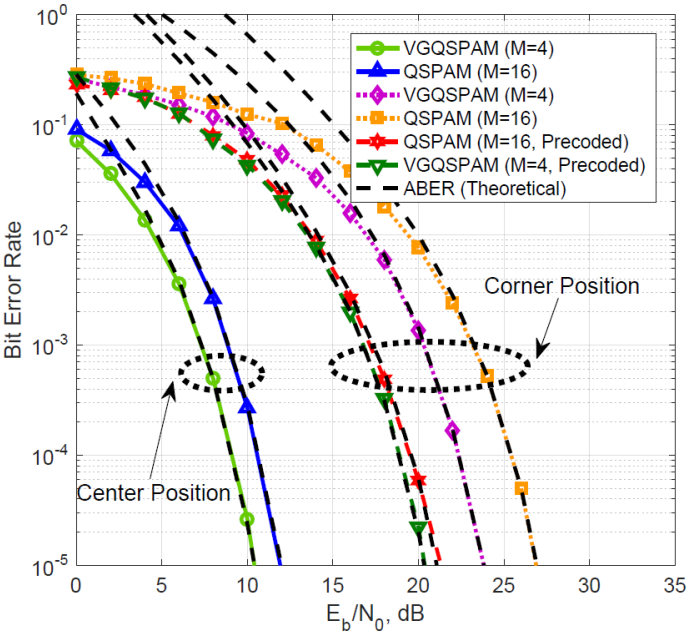

Figure 4. BER simulations and ABER theoretical results for 5 LEDs in two different Rx positions at a spectral efficiency of 5 bits/sec/Hz.

The complexity of the proposed schemes is determined by obtaining the total number of real multiplications and divisions on the receiver [14]. In the case of ML receiver, $\left|\left|\mathbf{y} - \mathbf{HWx}\right|\right|_{\mathrm{F}}^{2}$ requires four real multiplications. These operations are realized N_r times and over the set of all possible $\mathbf{x}$ vectors. Thus, the complexity of the proposed schemes is equal to $6N_r2^{2SE}$. As a benchmark, spatial PAM (SPAM) has a receiver complexity of $2N_r2^{SE}$ [7].

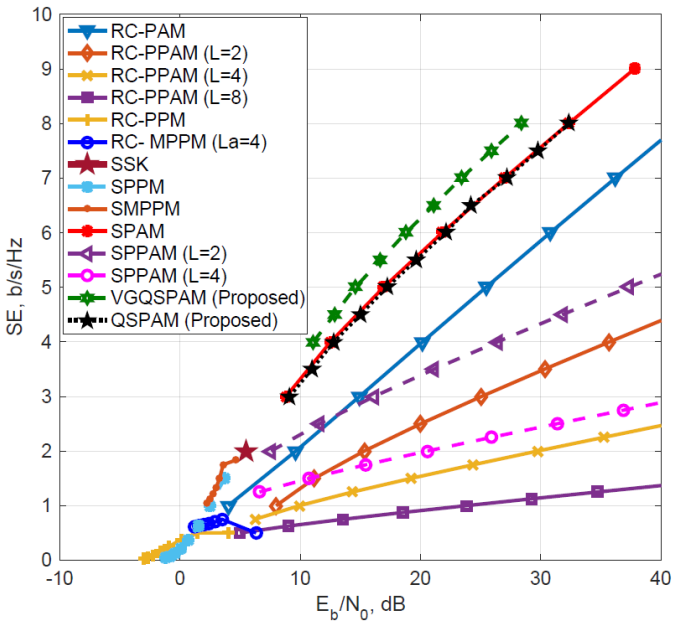

Figure 5. Required SE versus required electrical SNR for 4 LEDs at an SER value of 10^{-5} when Rx is placed in the center of the room.

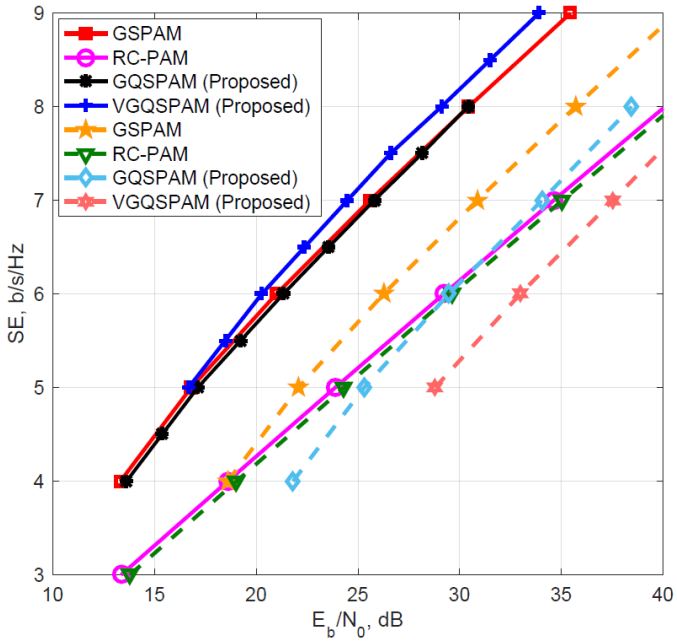

Figure 6. Required SE versus required electrical SNR for 5 LEDs at an SER value of 10^{-5} and N_a =2 (Solid lines are for center position and dashed lines are for corner position).

Table 3. The Diagonals of Precoding Matrices for Corner Position.

Modulation	Precoding Vector (**w**)	Channel Matrix (**H**)
QSPAM (N_t=4)	[0.42 1.15 1.15 1.08]	$\begin{bmatrix} 0.78 & 0.17 & 0.17 & 0.12 \\ 0.61 & 0.16 & 0.06 & 0.05 \\ 0.30 & 0.06 & 0.06 & 0.05 \\ 0.61 & 0.06 & 0.16 & 0.05 \end{bmatrix}$
VGQSPAM (N_t=4)	[0.47 1.20 1.20 0.94]	$\begin{bmatrix} 0.78 & 0.17 & 0.17 & 0.12 \\ 0.61 & 0.16 & 0.06 & 0.05 \\ 0.30 & 0.06 & 0.06 & 0.05 \\ 0.61 & 0.06 & 0.16 & 0.05 \end{bmatrix}$
GQSPAM (N_t=5, N_a=2)	[0.79 1.28 1.40 0.84 0.15]	$\begin{bmatrix} 0.82 & 0.16 & 0.24 & 0.16 & 0.11 \\ 0.77 & 0.06 & 0.08 & 0.16 & 0.05 \\ 0.39 & 0.06 & 0.08 & 0.06 & 0.04 \\ 0.77 & 0.16 & 0.08 & 0.06 & 0.05 \end{bmatrix}$
VGQSPAM (N_t=5)	[0.90 1.20 0.14 1.08 1.20]	$\begin{bmatrix} 0.82 & 0.16 & 0.24 & 0.16 & 0.11 \\ 0.77 & 0.06 & 0.08 & 0.16 & 0.05 \\ 0.39 & 0.06 & 0.08 & 0.06 & 0.04 \\ 0.77 & 0.16 & 0.08 & 0.06 & 0.05 \end{bmatrix}$

3. Results and Discussion

3.1. Simulation Results

BER simulation results and upper bound ABER curves are shown in Fig. 3 and Fig. 4 for the proposed QSPAM, GQSPAM, and VGQSPAM schemes. The least correlated channel is obtained in the center of the room and the most correlated channel is at the corners. Therefore, two positions have been considered to achieve the best and worst BER performances. In Fig. 3, QSPAM and VGQSPAM results are presented for an indoor scenario with 4 LEDs at a SE of 4 bits/sec/Hz; GQSPAM is not considered in this scenario because it has the same structure as QSPAM. Due to the less correlated channel matrix, the BER performance of the schemes increases in the center of the room and precoding provides significant performance improvement for the corner position. VGQSPAM has the best BER performance for all cases in this scenario. In Fig. 4, BER results are shown for 5 x 4 indoor MIMO VLC scenario at a SE of 5 bits/sec/Hz. When the Rx is in the center position, VGQSPAM performs better than GQSPAM. However, due to the increased correlation, GQSPAM has the best performance in the corner position.

SE versus required electrical SNR results are presented in Fig. 5 and Fig. 6 for 4 x 4 and 5 x 4 MIMO VLC, respectively. In these figures, the symbol error rate (SER) value is considered to be 10^{-5}, and Rx is placed in two different positions. As a benchmark, well-known pulse modulation schemes, namely PAM, PPM, PPAM are considered with MIMO techniques [18-20]. Here, PPM and PPAM are poor in terms of SE due to their high bandwidth requirements and repetition coding (RC) cannot take advantage of the spatial domain. However, SPAM and generalized SPAM (GSPAM) provide significant SE performance for the considered scenarios. When Rx is placed in the center of the room, VGQSPAM outperforms SPAM and GSPAM for two different Tx setup (Nt = 4 and Nt = 5). The main reason for this is the low channel correlation. GSPAM performs better in the corner position and outperforms RC schemes at higher SE values.

4. Conclusions and Recommendations

In this letter, indoor MIMO VLC scenarios close to real conditions are designed and new quadrature spatial schemes are proposed. The proposed QSPAM scheme and its generalized versions, namely GQSPAM, VGQSPAM, efficiently use the spatial domain for MIMO VLC. VGQSPAM performs better than benchmarks in less correlated channel conditions, but VGQSPAM performance decreases with increasing correlation. Consequently, proposed schemes take advantage of the spatial domain with an increasing number of LEDs and can be a good solution for less correlated MIMO VLC systems.

References

[1] Zeng L., et al. 2009. High data rate multiple input multiple output (MIMO) optical wireless communications using white led lighting, IEEE Journal on Selected Areas in Communications, 27, 9, pp. 1654–1662. https://doi.org/10.1109/JSAC.2009.091215

[2] Di Renzo, M., Haas, H., Ghrayeb, A., Sugiura S., and Hanzo, L. 2014. Spatial Modulation for Generalized MIMO: Challenges, Opportunities, and Implementation, Proceedings of the IEEE, 102, 1, pp. 56–103. https://doi.org/10.1109/JPROC.2013.2287851

[3] Mesleh, R., Ikki S. S., and Aggoune, H. M. 2015. Quadrature Spatial Modulation, IEEE Trans. Vehicular Tech., 64, 6 pp. 738–742. https://doi.org/10.1109/TVT.2014.2344036

[4] Mesleh, R., Hiari, O., Younis, A. 2018. Generalized space modulation techniques: Hardware design and considerations, Physical Communication, 26, pp.87-95. https://doi.org/10.1016/j.phycom.2017.11.009

[5] Castillo-Soria, F. R., Cortez-González, J., Ramirez-Gutierrez, R., Maciel-Barboza F. M., and Soriano-Equigua, L. 2017. Generalized quadrature spatial modulation scheme using antenna grouping, ETRI Journal, 39, 5, pp. 707-717. https://doi.org/10.4218/etrij.17.0117.0162

[6] Hussein, H. S., and Elsayed, M. 2018. Fully-Quadrature Spatial Modulation, IEEE International Black Sea Conference on Communications and Networking

(BlackSeaCom), Batumi, pp. 1-5. https://doi.org/10.1109/BlackSeaCom.2018.8433718

[7] Celik, Y., and Colak, S. A. 2020. Quadrature spatial modulation sub-carrier intensity modulation (QSM-SIM) for VLC, Physical Communication, 38, pp. 1-10. https://doi.org/10.1016/j.phycom.2019.100937

[8] Dimitrov, S. and Haas, H. 2015. Principles of LED Light Communications, Cambridge University Press, Cambridge, UK.

[9] Barry, J. R. 1994. Wireless Infrared Communications, Norwell, MA Kluwer.

[10] Islim, M. S. and Haas, H. 2016. Modulation Techniques for Li-Fi, ZTE Communications, 14, 2, pp. 29-40. https://www.research.ed.ac.uk/portal/en/publications/modulation-techniques-for-lifi

[11] Nuwanpriya, A., et. al. 2015. Indoor MIMO visible light communications: Novel angle diversity receivers for mobile users, IEEE Journal on Selected Areas in Communications, 33, 9, pp.1780-1792. https://doi.org/10.1109/JSAC.2015.2432514

[12] Lee, K., Park, H., and Barry, J. 2011. Indoor Channel Characteristics for Visible Light Communications, IEEE Commun. Lett., 15, 2, pp. 217-219. https://doi.org/10.1109/LCOMM.2011.010411.101945

[13] Fath, T. and Haas, H. 2013. Performance comparison of MIMO techniques for optical wireless communications in indoor environments, IEEE Transactions on Communications, 61, 2, pp. 733–742. https://doi.org/10.1109/ TCOMM.2012.120512.110578

[14] Mesleh, R., and Alhassi, A. 2018. Space Modulation Techniques, Hoboken, NJ, USA:Wiley.

[15] Lee, M.C., Chung, W.H., and Lee, T.S. 2015. Generalized precoder design formulation and iterative algorithm for spatial modulation in MIMO systems with CSIT, IEEE Trans. on Comm., 63, 4, pp. 1230-1244. https://doi.org/10.1109/TCOMM.2015.2396521

[16] Cheng, P., and et al. 2018. A unified precoding scheme for generalized spatial modulation, IEEE Trans. on Comm., 66, 6, pp. 2502-2514. https://doi.org/10.1109/TCOMM.2018.2796605

[17] Grant, M. and Boyd., S. 2013. CVX: Matlab software for disciplined convex programming, version 2.0 beta. http://cvxr.com/cvx

[18] Zhang, H. and Gulliver, T.A. 2005. Pulse position amplitude Modulation for time-hopping multiple-access UWB communications, in IEEE Transactions on Communications, 53, 8, pp. 1269-1273.

[19] Olanrewaju, H.G., Thompson, J., and Popoola, W.O. 2016. On spatial pulse position modulation for optical wireless communications, 2016 IEEE Photonics Society Summer Topical Meeting Series (SUM), pp. 44-45. https://doi.org/10.1109/PHOSST.2016.7548717

[20] Alaka, S. P., Narasimhan, T., and Chockalingam, A. 2015. Generalized Spatial Modulation in Indoor Wireless Visible Light Communication, IEEE Global Communications Conference (GLOBECOM), pp. 1-7. https://doi.org/10.1109/GLOCOM.2015.7416970